



A CR-5G network based on multi-user for various waveforms detection

Waleed Algriree ^{a,*}, Nasri Sulaiman ^{a,*}, Maryam Isa ^a, Ratna K.Z. Sahbudin ^b, Siti L.M. Hassan ^c, Emad Hmood Salman ^d, Mokhalad Alghrairi ^a



^a Department of Electrical and Electronic Engineering, Faculty of Engineering, Universiti Putra Malaysia, Serdang, Selangor 43400, Malaysia

^b Department of Computer and Communication Systems Engineering, Faculty of Engineering, Universiti Putra Malaysia, Serdang, Selangor 43400, Malaysia

^c Faculty of Electrical Engineering, Universiti Teknologi MARA, Selangor, Malaysia

^d Department of Communications Engineering, College of Engineering, University of Diyala, Diyala, Baquba 32001, Iraq

ARTICLE INFO

Article history:

Received 17 December 2021

Revised 21 April 2022

Accepted 22 May 2022

Available online 31 May 2022

Keywords:

Cooperative spectrum sensing

Detection performance

F-OFDM-5G

FBMC-5G

SNR wall

UFMC-5G

ABSTRACT

The 5G network is promised to provide all the requirements surfacing from the speedily rising number of mobile phone users rather than huge amount of data transmission. Many 5G waveforms can be used by 5G network such as Filtered-Orthogonal Frequency Division Multiplexing (F-OFDM), Universal Filtered Multi-Carrier (UFMC), or Filter Bank Multi-Carrier (FBMC) waveform. To effectively capitalize on the spectrum resources, Internet of Thing (IoT), and multimedia transmission, the Cooperative Spectrum Sensing (CSS) system is being extensively utilized by Cognitive Radio (CR). It is able to meet the requisite communication services, however, the conventional CSS systems have been designed to detect only single kind of 5G waveform and poor detection performance for low signal-to-noise ratio (SNR). In this paper, a hybrid filter based CSS system is proposed for detection of various 5G waveforms by multi-user. The proposed filter includes three cascaded stages: cosine filtering, Welch segmentation, and Hamming windowing. The proposed detection system is applied on different data such as various of waveforms and SNRs. The simulation results exhibit a significant detection performance for the parameters of less than zero dB of SNR, greater than 95% global detection probability, less than 1% global system error probability, and less than 1% global false alarm probability. In addition, the detection performance reveals that the proposed system is outperformed related works as shown in the comparison in terms of the previous parameters.

© 2022 THE AUTHORS. Published by Elsevier BV on behalf of Faculty of Computers and Artificial Intelligence, Cairo University. This is an open access article under the CC BY-NC-ND license (<http://creativecommons.org/licenses/by-nc-nd/4.0/>).

1. Introduction

Lately, upcoming 5G wireless systems exploit different types of filters and windows to provide high flexibility since the previous ones suffer from limited flexibility and the unfavorable coexistence for various channel conditions. To efficiently manage the diversity

of usage scenarios, an adaptable allocation of available resources of time-frequency is required. Even though OFDM has been utilized in long-term evolution advanced (LTE-advanced) and 5G, it is still crucial to examine the alternative filtered-based strategies which meet the previously mentioned design needs for upcoming wireless systems, like Universal filtered multi-carrier (UFMC), filtered orthogonal frequency division multiplexing (F-OFDM), and filter bank multi-carrier (FBMC). Contrary to OFDM, FBMC uses a filtering functionality to every sub-band which has more than single subcarrier. FBMC and F-OFDM provide the lower OOB (out-of-band) emission and improved time/frequency localization characteristics. UFMC method applies sub-band-wise filtering to lessen OOB. Thus, the filters are shorter in comparison to the FBMC, in which the filter length is much longer with respect to the symbol duration [1–4].

Unluckily, with the introduction of the 5th generation wireless networks (5G) era, the band access mobile devices can lead to scarcity of spectrum resources. The registered spectrum always displays low utilization, and existent resources are not utilized efficiently. Cognitive radio (CR) as a promising technology has been proposed

* Corresponding authors.

E-mail addresses: wkh_portsmouth@yahoo.com (W. Algriree), nasri_sulaiman@upm.edu.my (N. Sulaiman), maryam@upm.edu.my (M. Isa), ratna@upm.edu.my (R.K.Z. Sahbudin), sitailalutul.mohdhassan@yahoo.com (S.L.M. Hassan), emad_salman_eng@uodiyala.edu.iq (E. Hmood Salman), mokhaladkha-leel@gmail.com (M. Alghrairi).

Peer review under responsibility of Faculty of Computers and Information, Cairo University.



Production and hosting by Elsevier

to offer high spectrum utilization, wherein Secondary Users (SUs) are permitted to gain access to the spectrum when there is no Primary User (PU). Spectrum sensing (SS) technique can achieve improved sensing operation when the probability of detection (P_d) is greater while the false alarm probability (P_f) is lower. Nonetheless, SS will use some system resources and reduce its performance [5,6]. As far as the significance of the radio scene analysis function is concerned, basic spectrum sensing techniques display several limitations. Hidden node problems, shadowing, etc. always render spectrum sensing demanding. A PU transmission may be unnoticeable for a CR sensing terminal, even if its signal is entirely usable by a neighboring PU receiver. With the aim to make the spectrum sensing operation reliable and effective, and to stabilize both hidden node and multipath problems, Cooperative Spectrum Sensing (CSS) is regarded as a vital solution specifically in wideband situations. It involves two or more collaborative radio receivers in decision making at the time of the spectrum sensing [7].

The literature mentions different schemes that have employed the CSS scheme. However, all these schemes have been employed to sense just one type of 5G waveforms. Some of these are employed for various types of mappers as well as modulation. Evaluation of the performance results was done based on probabilities of detection, false alarm as well as miss detection. In 2017, a multi-modal system was proposed by Liu X. et al. [8] with regards to CSS scheme. The proposed system comprises spectral, energy and waveform detectors that have been applied for each SU. The tested channels include Additive White Gaussian Noise (AWGN) as well as fading for 5G communications system, while the Bayesian fusion algorithm is employed to provide the decision. For high numbers of SUs with desired results, the sensing performance is carried out; however, it is not suitable for low Signal-to-Noise Ratio (SNR). In 2019, for CSS scheme, Kumar A., and Saha S. [9] evaluated the log likelihood ratio-based energy detection model. Every SU includes multiple sensing antenna (2–10) as well as two transmitting antenna, while the Fusion Center (FC) includes multiple receiving antenna (2–10). The studied model has been used on Multi-Input-Multi-Output (MIMO) channel to minimize the computational complexity. Unfortunately, the probability pertaining to false alarm is not low, while it is high for the SNR wall. In the same year, a deep CSS algorithm was developed by Lee W. and Cho D. [10] as per the convolutional neural networks. The developed algorithm can effectively identify the frequency vacant in a 5G network. It is employed to determine the optimal value pertaining to K , thus providing the best K -out-of- N rule. The performance is optimum for 32 SUs; however, for low SNR, it is poor. In the previous year, an adaptive double-threshold CSS algorithm was designed by Yu S. et al. [11] for the ED approach. The upper and lower levels of threshold can be adjusted with the designed algorithm in terms of weighting thresholds pertaining to each SU. For SNR in the range from –20 dB to 10 dB, the AWGN type channel is employed. For low SNR, the performance achieved is significant (high detection probability); however, for SNR <–15 dB and only 25 SUs, the performance is weak. In the current year, Balachander T., and Krishnan M. [12] evaluated the Cognitive Radio Network (CRN) scheme based on the 5G system. The employed SS scheme was based on CSS with MIMO transmission system through AWGN as well as Rayleigh fading channel types. Only for 10 SUs, the detection performance is desirable with regards to high SNR. However, the proposed system's performance is poor when it comes to low SNR. In the same year, a CSS scheme was designed by Giri M.K. and Majumder S. [13] by regarding the Kernel fuzzy c-means clustering model. Comparison of this model is done with eigenvalues pertaining to the signal covariance matrix-based spectrum sensing. The designed system has been performed only for 12 SUs with precise detection; however, its computational complexity level is deemed to be high and is unable to sense for SNR with the value

lesser than –10 dB. In 2021, a composite two-tier threshold algorithm was proposed by Kansal P., Gangadharappa M., and Kumar A. [14] with regards to the CSS scheme that uses the confusion region. The proposed algorithm has also been used for the 5G system with sub-6 GHz. Significant results were achieved with the detection performance due to low error and short sensing time for 50 SUs. Nonetheless, the put forward system is deemed unsuitable for SNR less than 0 instead of its complexity. A hybrid algorithm was also proposed by Gupta V. et. al. [15] by considering the particle swarm optimization as well as whale optimization algorithm, in which the particle swarm optimization was employed to enhance the whale optimization algorithm. The hybrid algorithm has been used for CSS scheme in the 5G system. Even though the performance results are not desirable, sensing by the hybrid system is done accurately. For a few SUs, even though the probability of false alarm is not low, the hybrid system was unable to deal with low SNR. In the current year, a truncated Gaussian distribution is considered a channel by authors to study CRN [16]. They proposed the energy detection algorithm for single SU with majority rule for CSS to face the SNR wall. The detection performance of proposed algorithm is obtained 0.94 detection probability with 0.1 false alarm probability. However, it failed to sense for SNR <–17 dB with only 5 SUs. In 2022 too, the authors in [17] are proposed a sensing algorithm according to the Eigenvalue extraction and Maximum Entropy Fuzzy clustering (EMEF). Rayleigh flat fading is supposed a channel whereas the noise is considered a circularly symmetric complex Gaussian distribution. For 4 SUs and –8 dB SNR, the performance of sensing is obtained 0.97 detection probability with 0.1 false alarm probability. Nonetheless, the proposed algorithm is failed for short length of received PU signal and low SNR.

Nevertheless, the aforementioned CSS methods are used in a network with only single type of 5G waveform with undesirable detection performance especially in low SNR case. Moreover, every method from the previous CSS methods can detect only one kind of 5G waveforms, i.e., it fails to detect other necessary kinds of 5G waveforms. In this paper, a new CSS method based on Cosine-Welch-Hamming cascaded hybrid filter is designed. This filter can detect various kinds of 5G waveforms, which are UFMC, F-OFDM, and FBMC, where are used in 5G network. Furthermore, the proposed filter can overcome other issues such as high SNR variance, different signal length, and various specifications of kinds of waveforms. The proposed filter includes three stages; cosine filtering, Welch periodogram, and Hamming windowing. The first stage function is identifying the traffic of the received PU signal, while the second stage function is segmenting the resulted traffic signal into overlapped segments to decrease the noise variance. Finally, the function of the Hamming windowing is conserving the signal quality, that may be influenced, by the periodogram by applying it on every segment. Thus, a Power Spectral Density (PSD) for every segment is obtained, then averaging PSDs, to compare with the predefined threshold of received PU signal to produce the decision. The main contributions of the proposed filter can be summarized as follows:

- The proposed filter is derived principally then applied on 5G network based CRN to sense different kinds of 5G waveforms such as UFMC, F-OFDM, and FBMC waveforms.
- The proposed filter did not take long to sense as it compressed the sensed signal, where it preserved the resolution of the sensed signal and reduced the noise difference.
- The proposed filter damps the high SNR variance i.e.; it can detect various signals for SNR less than zero dB. Moreover, it achieves greater sensing accuracy, reduced sensing error, and greater sensing performance in comparison to the similar methods.

The rest of the paper is structured as follows: [Section 2](#) illustrates the mathematical signal framework for the 5G waveforms; UFMC, F-OFDM, and FBMC, and describes the CSS composition. [Section 3](#) describes the derived closed form for the mathematical framework of the proposed Cosine-Welch-Hamming hybrid filter and expresses this framework for all waveform types. [Section 4](#) examines the theoretical performance (graphically and numerically) of the presented technique with respect to sensing performance, computational complexity, low SNR, various bit rates, and error detection system, by comparing it to some similar works. [Section 5](#) presents the conclusion.

2. Preliminaries of 5G waveforms and CSS system

2.1. Waveforms formulation based 5G

For more than a decade, OFDM has been used for wireless standards and broadband wired standards. Currently, OFDM is employed for a broad class of discrete multi-tone transmission (DMT) standards, e.g., digital video broadcasting cable (DVB-C) and asymmetric digital subscriber line (ADSL). Because of the merits pertaining to the orthogonality, the orthogonal subcarriers that are closely spaced help in partitioning the bandwidth that is available into a group of narrow subcarriers. In addition, the adaptive modulation schemes could be used for subcarrier bands to improve the overall bandwidth efficiency. Robust multi-path fading, high data rate transmission as well as ease of implementation are offered by OFDM.

The OFDM is responsible for partitioning the transmission bandwidth into a group of orthogonal subcarriers. Representation of a general OFDM signal could be done as:

$$s(t) = \sum_{n=-\infty}^{\infty} s_n(t - nT) \quad (1)$$

here, $s(t)$ denotes the transmitted signal, T denotes the OFDM symbol duration, and $s_n(t)$ signifies the n -th OFDM symbol pertaining to a downlink slot, which can be presented as:

$$s_n(t) = \sum_{k=0}^{K-1} a_{n,k} \delta(t) v(t) e^{j2\pi k \Delta f t} = \sum_{k=0}^{K-1} a_{n,k} v(t) e^{j2\pi k \Delta f t} \quad (2)$$

here, $\delta(t)$ represents the Dirac delta impulse, K indicates the number of subcarriers, k signifies the subcarrier index, $v(t)$ denotes a pulse shape (or prototype filter), Δf represents the subcarrier spacing $a_{n,k}$ signifies the complex data symbol pertaining to the k th subcarrier and n th OFDM symbol. With regards to the conventional OFDM, the pulse shape $v(t)$ can be considered as a rectangular pulse possessing width T . Thus, the OFDM signal can be derived based on Equations [\(1\)](#) and [\(2\)](#) as follows [\[18\]](#):

$$s(t) = \sum_{n=-\infty}^{\infty} s_n(t - nT) = \sum_{n=-\infty}^{\infty} \sum_{k=0}^{K-1} a_{n,k} v(t - nT) e^{j2\pi k \Delta f (t - nT)} \quad (3)$$

In terms of the waveform candidate for 5G communication systems, FBMC is regarded to be a frontier, where numerous studies have highlighted the benefits pertaining to it. The filter bank can be defined as an array of filters, which can also be applied to every K subcarrier. $v(t)$ can be defined as the prototype filter, and mathematical representation of the FBMC signal is done as [\[19\]](#):

$$\begin{aligned} s(t) &= \sum_{n=-\infty}^{\infty} \sum_{k=0}^{K-1} a_{n,k} \delta(t - nT) v(t) e^{j2\pi k \Delta f (t - nT)} \\ &= \sum_{n=-\infty}^{\infty} \sum_{k=0}^{K-1} a_{n,k} v(t - nT) e^{j2\pi k \Delta f (t - nT)} \end{aligned} \quad (4)$$

Other 5G waveform i.e., F-OFDM has become a key candidate. F-OFDM still employs OFDM as its key waveform as well as sub-band filters for every sub-band that possesses greater than one subcarrier. For unified expression, it is assumed that applying of spectrum shaping filter $h(t)$ is done on the entire passband, which means that the total number of sub-bands is one [\[20\]](#).

$$s(t) = \sum_{n=-\infty}^{\infty} \left\{ \left[\sum_{k=0}^{K-1} a_{n,k} e^{j2\pi k \Delta f (t - nT)} \right] \otimes h(t - nT) \right\} \quad (5)$$

The last but not least, UFMC waveform candidate of 5G provides filtering at a sub-band level to decrease OOB. Sub-bands are used to split the bandwidth, and filters are implemented using a fixed frequency-domain level. Assuming that there are B sub-bands, the UFMC baseband waveform for filter length L can be expressed as [\[11\]](#):

$$S[k] = \sum_{b=0}^{B-1} \sum_{l=0}^{L-1} \sum_{n=0}^{N-1} d_n^b g[l] e^{j2\pi k \frac{(n-l)}{N}} \quad (6)$$

where d_n^b denotes the complex data transfer corresponding to the b -th sub-band and n -th subcarrier; $g[l]$ denotes the frequency version of the windowing expression corresponding to the time domain finite impulse response (FIR) filter.

2.2. CSS model background

The decision system has a vital function in the cooperative spectrum sensing approach, especially during the second phase. It obtains the detection data from numerous cognitive relays, and decision-making is based on fusion, requiring several results. The fundamental assumption concerning the binary-outcome spectrum sensing detection is [\[9,21\]](#):

$$x(t) = \begin{cases} w(t) & : H_0 \\ s(t) + w(t) & : H_1 \end{cases} \quad (7)$$

where $s(t)$ and $w(t)$ denote the transmitted signal (as defined before) and noise, respectively. H_0 and H_1 represent the null and alternate hypotheses. Signal transmission from primary to secondary users help the latter implement spectrum sensing. Every secondary user transmits a bit concerning the detection outcome to the center. Decision fusion is implemented at the center to consider the outcomes from all users and implement a voting mechanism by using OR rule to define the primary user presence. This research comprises user-specific P_d and P_f values because sensing locations are different. The probability values can be expressed as [\[22\]](#)

$$P_f = \text{Prob}\{(H_1 | H_0)\} = Q\left(\frac{\eta - \sigma_w^2}{\sqrt{\frac{2}{N}} \sigma_w^2}\right) \quad (8)$$

$$P_d = \text{Prob}\{(H_0 | H_1)\} = Q\left(\frac{\eta - (\sigma_w^2 + \sigma_s^2)}{\sqrt{\frac{2}{N}} (\sigma_w^2 + \sigma_s^2)}\right) \quad (9)$$

where N and η represent the target signal length and decision limit, signal and noise power levels are represented using σ_s^2 and σ_w^2 . The detection performance metric that indicates the detection probability against false alarm probability is called the Receiver Operating Characteristic (ROC). ROC values are ideal for high detection probability (greater than 90%) and low false alarm probability (smaller than 10%). The present subsection uses the ROC metric for global likelihood values concerning detection and false alarms.

Considering decision fusion implementation using the OR scheme for M secondary users, the following can be expressed.

$$Q_f = 1 - \prod_{m=1}^M (1 - P_f) \quad (10)$$

$$Q_d = 1 - \prod_{m=1}^M (1 - P_d) \quad (11)$$

where Q_f and Q_d denote the global probability values for false alarm and detection.

3. Proposed system of CR-5G network

3.1. CR-5G network architecture

The typical CR system includes a base station (BS), PU, and M SUs. The frame concerning the CR-5G overlay using tri-waveform transmissions is depicted in Fig. 1. Here, the F-OFDM waveform is depicted; local decisions are indicated using sequential arrows, while dashed arrows denote FBMC-specific local decisions. Moreover, UFMC local decisions are indicated using the dash-dot notation. There are several PU waveforms in a 5G network implementation; the SUs read channel characteristics concurrently for every waveform type. In the present scenario, SU sensing is followed by local decision-making concerning all waveform types. These decisions are communicated to FC because the PU might rely on many transmission types. As specified previously, the CSS approach is suggested to enhance detection using cooperative PU sensing at the SU level. The CSS approach comprises a fusion station implementing SU management and sensing data exchange. The FC works as a base location for a centralized CR implementation. It gathers and records SU-specific local decision data. The center uses several combinations of the sensed data sets to arrive at a decision transmitted to every SU. The FC connects to SUs using a control channel. The SUs upload sensing and status data to the fusion station at specific intervals using the control channel uplink. Similarly, decision and control data are sent to the SUs using the downlink control channel [8].

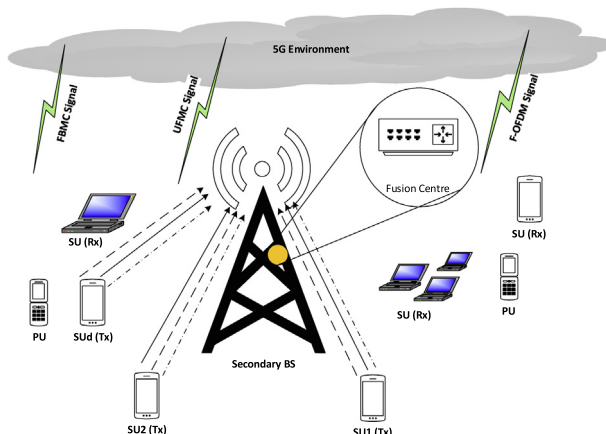


Fig. 1. The Proposed Model of Multi-User Various Waveforms Detection of CR-5G Network.

3.2. Proposed model analyzing

The CSS approach suggested in this research uses a hybrid filter for potential 5G waveforms depicted in Fig. 2 of this section. The filter used for this study processes the 5G waveform using the cosine filter to implement energy monitoring using SS frequency domain approach, as specified in the below-mentioned equations. The first step processes the signal using the cosine filter [23,24].

$$R[k] = \left(\frac{(-1)^k}{\sqrt{2}} r[0] + \sum_{v=0}^{V-1} r[v] \cos \left(\frac{\pi k(2v+1)}{2V} \right) \right), \quad 0 \leq k \leq K-1 \quad (12)$$

where, $r[v]$ denotes the 5G waveform corresponding to length V . It is specified below:

$$r[v] = \begin{cases} w[v] & H_0 \\ \begin{cases} s_{F_OFDM}[v] \\ s_{UFMC}[v] \\ s_{FBMC}[v] \end{cases} + w[v] & H_1 \\ & v = 1, 2, \dots, V \end{cases} \quad (13)$$

where $w[v]$ denotes Gaussian noise having zero mean and a σ_w^2 variance. The noteworthy point is that the received 5G signals belonged to the s_{F_OFDM} , s_{UFMC} , or s_{FBMC} kind. Moreover, the assumption was that the signals were independent and used identically distributed (i.i.d) random technique having σ_s^2 variance and zero mean. The filtered signal corresponding to $r[v]$ is represented using $R[k]$.

The subsequent step comprises removing the null coefficients corresponding to $R[k]$ to reduce sensing duration by reducing computational needs. Therefore, K' is the updated $R[k]$ length, where $K' < K$ (i.e., $R'[k]$ is the $R[k]$ with K' length). Several samples are required for traffic movement. Cosine filter implementation was followed by splitting $R'[k]$ into N_{seg} segments, each having L_{seg} length, determined using the Welch segmentation approach. Consequently, PSD values are computed for every segment after isolating using the Hamming window technique. Finally, the overall PSD (RPSD) is considered the mean value of the prior PSDs; this value is used as the test statistic. The previous steps have been elaborated mathematically for F-OFDM, UFMC, and FBMC approaches, respectively.

Eq. (14) expresses the cosine-filter processed F-OFDM signal. Hence, Eq. (15) presents null coefficient elimination.

$$\begin{aligned} R_{F_OFDM}[k] = & (-1)^k \sum_{b=0}^{B-1} \sum_{m=0}^{M-1} \sum_{l=0}^{L-1} \sum_{n=0}^{N-1} \frac{s_{m,n}^b g_b[l]}{\sqrt{2}} + \\ & \sum_{v=0}^{V-1} \sum_{b=0}^{B-1} \sum_{m=0}^{M-1} \sum_{l=0}^{L-1} \sum_{n=0}^{N-1} s_{m,n}^b g_b[l] e^{j2\pi v(n-l-mC)/N} \cos \left(\frac{\pi k(2v+1)}{2V} \right), \quad 0 \leq k \leq K-1 \end{aligned} \quad (14)$$

$$R'_{F_OFDM}[k] = R_{F_OFDM}[k], \quad 0 \leq k \leq K'-1 \quad (15)$$

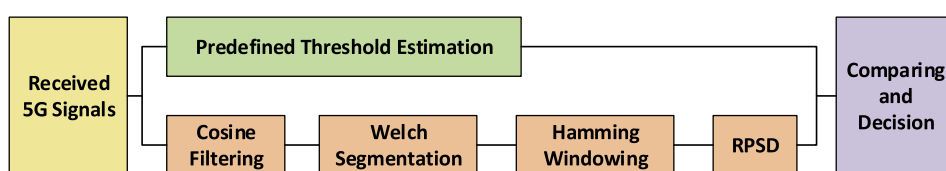


Fig. 2. The Proposed SS Technique for Various 5G Waveforms Detection Block Diagram.

Further, the processed UFMC waveform is specified to transform using Eqs. (16) and then (17) to reduce the length of the targeted signal.

$$\begin{aligned} R_{UFMC}[k] = & (-1)^k \sum_{b=0}^{B-1} \sum_{l=0}^{L-1} \sum_{n=0}^{N-1} s_n^b g[l]/\sqrt{2} + \sum_{v=0}^{V-1} \sum_{b=0}^{B-1} \sum_{l=0}^{L-1} \sum_{n=0}^{N-1} \\ & s_n^b g[l] e^{j2\pi v \frac{(n-l)}{N}} \cos\left(\frac{\pi k(2v+1)}{2V}\right), \\ 0 \leq k \leq K-1 \end{aligned} \quad (16)$$

$$R'_{UFMC}[k] = R_{UFMC}[k], \quad 0 \leq k \leq K'-1 \quad (17)$$

Eq. (18) expresses the changed FBMC waveform using the first stage; Eq. (19) expresses null coefficient elimination to keep the active samples.

$$\begin{aligned} R_{FBMC}[k] = & (-1)^k \sum_{m=-\infty}^{\infty} \sum_{n=0}^{N-1} s_{m,n} g\left[k - m \frac{N}{2}\right] e^{j\varphi_{m,n}} / \sqrt{2} \\ & + \sum_{v=0}^{V-1} \sum_{m=-\infty}^{\infty} \sum_{n=0}^{N-1} s_{m,n} g\left[k - m \frac{N}{2}\right] e^{j2\pi v \frac{n}{N}} e^{j\varphi_{m,n}} \cos\left(\frac{\pi k(2v+1)}{2V}\right), \\ 0 \leq k \leq K-1 \end{aligned} \quad (18)$$

$$R'_{FBMC}[k] = R_{FBMC}[k], \quad 0 \leq k \leq K'-1 \quad (19)$$

It is assumed that a $Ham[k]$ Hamming window operator (as depicted in Eq. (20)) is used for each segment based on the Welch segmentation approach as specified ahead [25],

$$Ham[k] = 0.54 - 0.46 \cos\left(\frac{2\pi k}{K}\right), \quad 0 \leq k \leq K-1 \quad (20)$$

$$PSD^{(j)}[k] = \frac{1}{L_{\text{seg}}} \left| \sum_{i=0}^{L_{\text{seg}}} R[i] Ham[i] \right|^2, \quad 0 \leq k \leq K-1, \quad j = 1, 2, \dots, N_{\text{seg}} \quad (21)$$

here, R' denoted $R'_{F\text{-OFDM}}$, R'_{UFMC} , or R'_{FBMC} . The mean PSDs are assessed in the following manner:

$$RPSD = \frac{1}{N_{\text{seg}}} \sum_{i=0}^{N_{\text{seg}}-1} PSD(i) = \lambda \quad (22)$$

Hence, the binary hypothesis for λ ($RPSD$) is:

$$\begin{cases} H_0, & \lambda \leq \eta \\ H_1, & \lambda > \eta \end{cases} \quad (23)$$

Moreover, Eq. (8) is used for determining P_f because it relies on the SNR and initial signal length. On the other hand, updated length K' is used to determine new P_d :

$$P_d = Q \left(\frac{\frac{\eta}{\sigma_w^2} - \vartheta \left(\frac{\sigma_s^2}{\sigma_w^2} + 1 \right)}{\sqrt{\left(\frac{2}{K'} \right) \vartheta \left(\frac{\sigma_s^2}{\sigma_w^2} + 1 \right)}} \right) \quad (24)$$

where

$$\vartheta = \frac{K}{K'} \quad (25)$$

From Eq. (24), the updated length K' is considered a crucial factor to obtain a better detection probability. In other words, when the detection probability is supposed to be 0.99, Eq. (24) is obtained an optimum rate of K' for given the predefined threshold and SNR.

In addition, the system error (global probability of error) can be expressed as

$$Q_e = 1 - Q_d + Q_f \quad (26)$$

where the global probability of detection has been obtained by using the new local probability of detection.

4. Simulation results and discussion

CSS fulfilment concerning the CR-5G framework is suggested for observing different waveform types like FBMC, F-OFDM, and UFMC in a 5G environment. The simulation of the proposed CSS system is set up by using MATLAB software that is performed by MathWorks®. In this simulation, the SNR is considered less than zero dB to test the detection performance of the proposed system in the difficult conditions. Moreover, one thousand trials are performed according to the Monte-Carlo approach. The waveform kinds are modulated with QAM mapper and other data of these kinds are specified below:

4.1. Impact of SNR on received signals

Here, the generated F-OFDM, UFMC, and FBMC waveforms have been presented using different SNR rates. They noted that the factor that significantly impacted the sensing performance of the system was the SNR, as the spectrum of every received F-OFDM, UFMC, and FBMC waveform signal was affected by SNR rates. Fig. 3 presents the PSDs of received F-OFDM waveforms that were generated using the SNR rates of (-30) dB, (-10) dB, and 10 dB. Thus, the noise variance (that was mixed with generated waveforms) for the (-30) dB SNR was the highest whereas the noise variance for 10 dB SNR was the lowest. As depicted in the figure, if noise variance was high, the PSD of the received F-OFDM signal was also high. Hence, the received F-OFDM signal with 10 dB SNR was the clearest, while the received F-OFDM signals having (-10) and (-30) dB SNR was not clear. Hence, the traffic estimation was affected by the SNR rates and needed an accurate sensing technique. The proposed sensing technique overcame this issue completely and could differentiate between the noise and traffic as presented in subsection 2.

Similarly, the received UFMC and FBMC waveforms show a higher PSD based on their SNR rates as presented in Figs. 4 and 5, respectively) these received UFMC and FBMC signals were generated using the SNR rates of (-30) dB, (-10) dB, and 10 dB (. The shape of the generated UFMC signal was different than that for the generated F-OFDM signal as it had a shorter length based

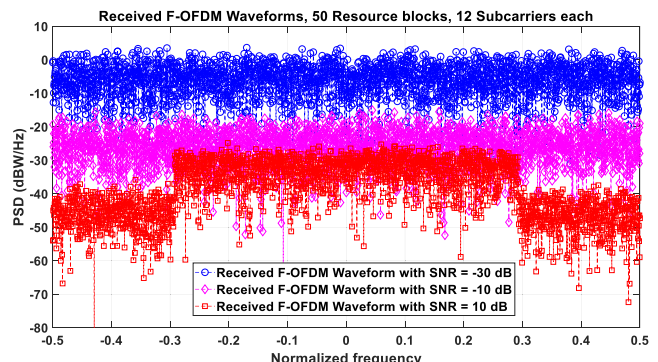


Fig. 3. The PSD of Received F-OFDM-5G for Various SNR Rates.

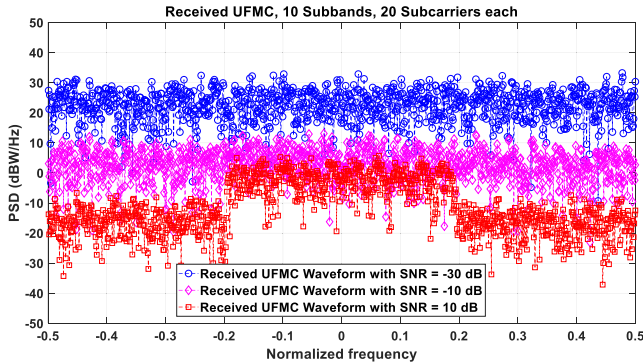


Fig. 4. The PSD of Received UFMC-5G for Various SNR Rates.

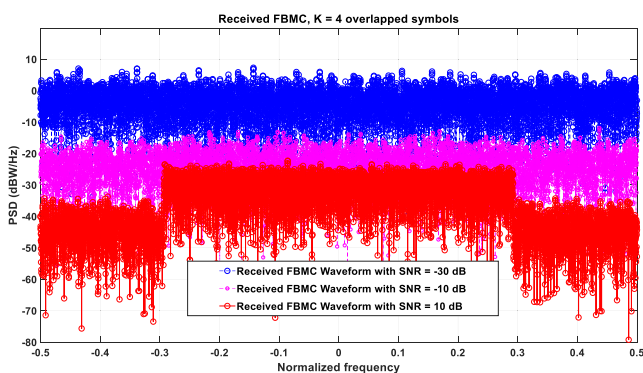


Fig. 5. The PSD of Received FBMC-5G for Various SNR Rates.

on the generating standards (**Table 1**). Hence, the proposed SS technique is able to decrease the effect of this problem.

To summarize, the generated 5G signals are unclear and it is difficult to differentiate them from the noise if the noise variance was high (for -10 dB and -30 dB SNR). Hence, the proposed technique could sense these signals and differentiate them from noise, as described in the section below.

4.2. Detection performance for F-OFDM-5G waveform

Figs. 6–8 depict the detection performance using -10 , -20 , and -30 dB SNR, respectively, for numerous SU values. Every curve in these figures represents the ROC between the global probabilities of detection and false alarm. **Table 2** reveals the best values of the global detection probability for 0.05 global false alarm probability and for various number of SUs. In addition, the rates of detection probability for $\text{SNR} < -20$ dB indicate that the updated length (1537 samples) is represented an optimum rate.

From **Fig. 6**, there are 1608 samples in the initial stream; however, the sensed stream comprises 1537 samples according to the proposed hybrid filter, which decrease the noise effect ($\text{SNR} = -10$ dB) to increase the local detection probability. Thus, it is observed that a higher SU count provides better performance; Q_d (for thirty SUs and fifty users) exceeds that only for ten users. Therefore, the global detection probability, Q_d is enhanced by increasing both of local detection probability and SUs number according to Eq. (11). In a similar manner, and for $\text{SNR} = -20$ dB, **Fig. 7** presents the performance levels that squeeze the initial stream to a 1524-sample stream. Enhanced performance is

obtained using a shorter sensed stream because the present case comprises a higher noise variance than the previous case. Although the SNR of the second case is lower, the global detection probability of the second case is better than that of the first case since the proposed hybrid filter damps the SNR affection and shorts the initial stream. Analogously, **Fig. 8** depicts performance levels for -30 dB SNR level. The new number of samples is 1522 according to the proposed hybrid filter and its performance is better than that of the first case. To enhance the global detection probability, even higher noise variance exists, shorting the sensed stream and increasing the SUs number are considered the most effect parameters, as shown in the comparison of the detection performance of the second and third cases.

Table 1
The data of Various 5G Waveforms.

F-OFDM	UFMC	FBMC
Number of FFT = 1024	Number of FFT = 512	Number of FFT = 1024
Number of Resource Block = 50	Size of Sub-band = 20	Number of Guard = 212
Number of sub-carriers = 12	Number of sub-bands = 10	Overlapping Symbols = 4
Length of cyclic prefix = 72	Length of cyclic prefix = 43	Number of Symbols = 100
Bits/Sub-carrier = 6	Bits/Sub-carrier = 4	Bits/Sub-carrier = 2
Tone offset = 2.5	Sub-band offset = 156	
Length of filter = 513	Length of filter = 43	
16 QAM	16 QAM	16 QAM

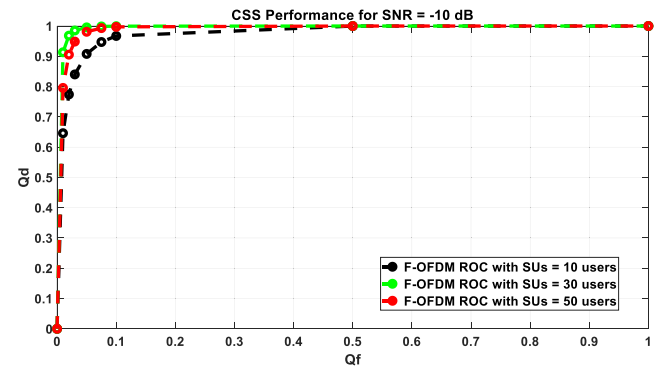


Fig. 6. F-OFDM Sensing for $\text{SNR} = -10$ dB.

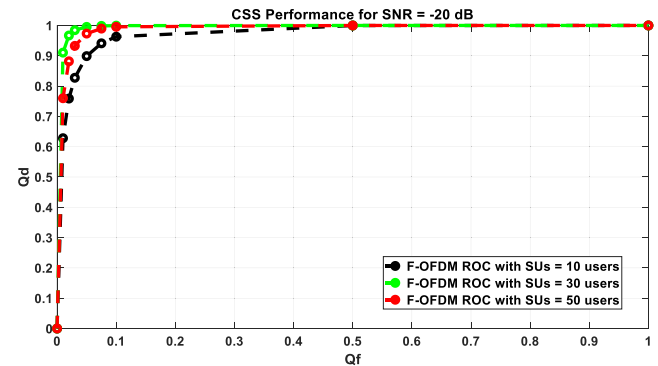


Fig. 7. F-OFDM Sensing for $\text{SNR} = -20$ dB.

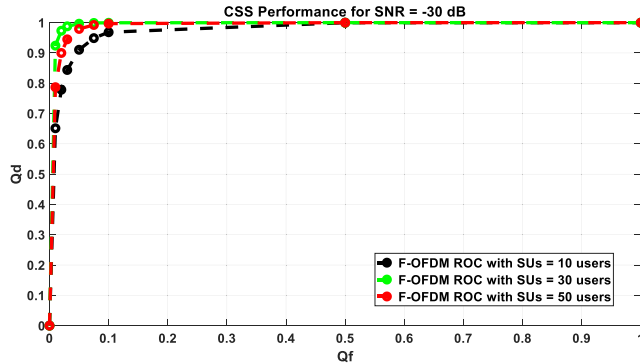
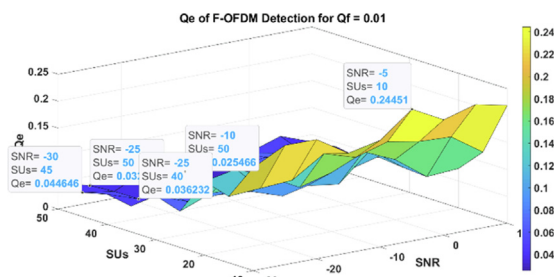
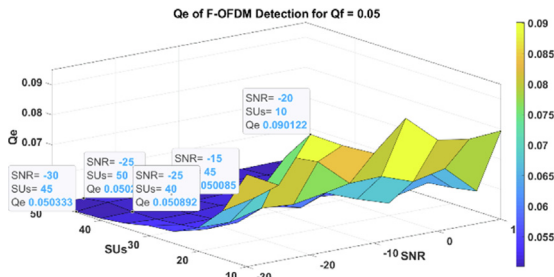
Fig. 8. F-OFDM Sensing for $\text{SNR} = -30 \text{ dB}$.

Table 2
 Q_d of F-OFDM-5G Waveform for Given Q_f , SNR, and SUs Ratios.

SUs No.	From Fig. 6	From Fig. 7	From Fig. 8
	SNR = -10 dB	SNR = -20 dB	SNR = -30 dB
10	$Q_d = 0.907$	$Q_d = 0.995$	$Q_d = 0.981$
30	$Q_d = 0.902$	$Q_d = 0.995$	$Q_d = 0.973$
50	$Q_d = 0.911$	$Q_d = 0.996$	$Q_d = 0.979$

Fig. 9. Q_e of F-OFDM for $Q_f = 0.01$.Fig. 10. Q_e of F-OFDM for $Q_f = 0.05$.

System error is a vital measure to determine the accuracy and efficacy of the formulated detection approach. A system error can be determined using detection-miss and false alarm probabilities. Figs. 9–12 correspond to system error of the F-OFDM sensing performance. In order to design a better detection performance, the global false alarm probabilities, Q_f are supposed to be as low as 0.01, 0.05, 0.07, and 0.1 for Figs. 9–12, respectively. In all figures, the global error probability is decreased with increasing the SUs number even the SNR was low since the proposed hybrid filter reduced the low SNR affection.

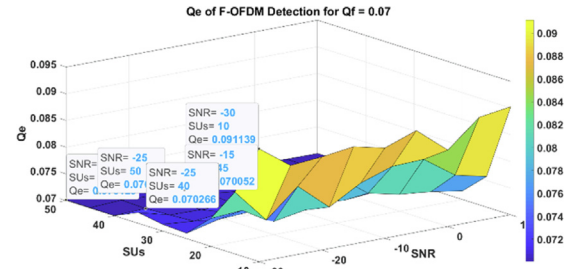
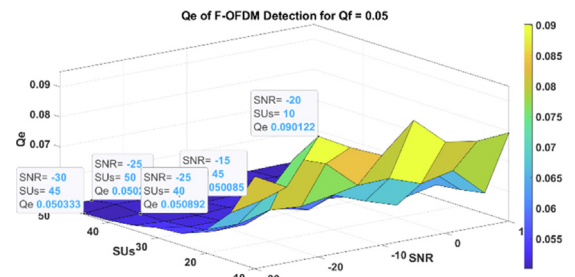
Fig. 11. Q_e of F-OFDM for $Q_f = 0.07$.Fig. 12. Q_e of F-OFDM for $Q_f = 0.1$.

Table 3 shows the lowest and the highest ratios of the global error probability for different values of the global false alarm probability, SNR, and SUs number. It can be see that the error is decreased once the SUs number is increased regardless the SNR, which is damped by using the hybrid filter.

4.3. Detection performance for UFMC-5G waveform

For UFMC-5G waveform kind, Figs. 13–15 show the performance of sensing using -10 , -20 , and -30 dB SNR, respectively. All ROC curves are obtained for a number of SUs. Table 4 depicts the best values of the global probability of detection for 0.05 global probability of false alarm. From this table, the updated length is 545 samples is considered an optimum rate since the probability of detection is the best rate.

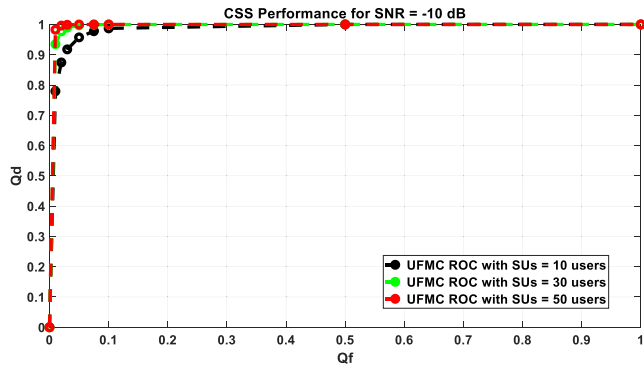
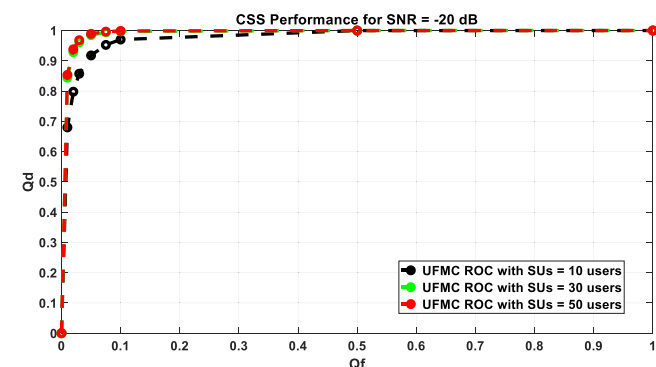
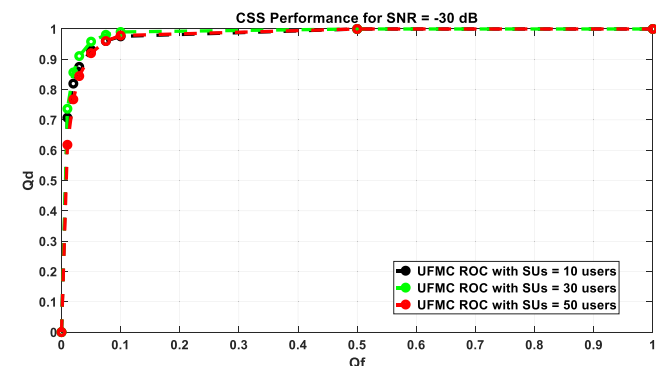
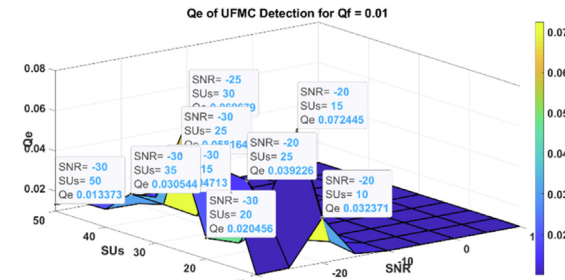
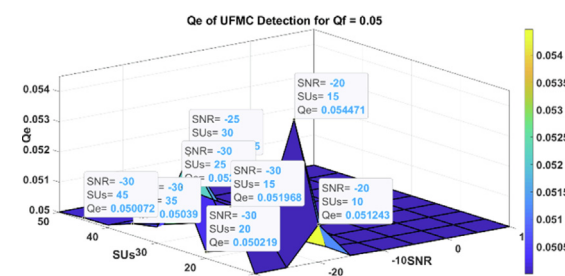
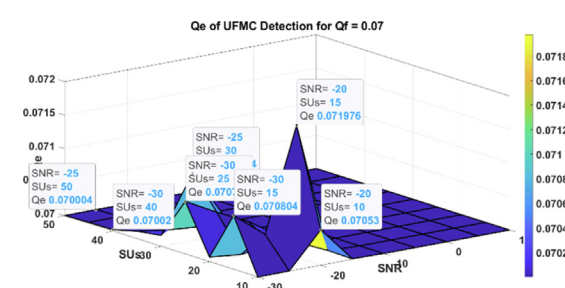
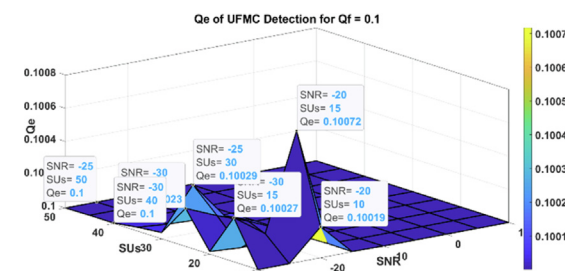
In Fig. 13, the ROC is performed for 545 samples, as against 554 in the initial stream for $\text{SNR} = -10 \text{ dB}$. Although the detection performance ratios are significant for different number of SUs, Q_d is better for 30 and 50 users. For $\text{SNR} = -20 \text{ dB}$, Fig. 14 presents the detection performance ranks that squeeze the initial stream to the 509 samples. the performance is also obtained as a significant rate but less than the previous case due to the SNR wall. Similarly, Fig. 15 depicts Q_d levels for -30 dB SNR with 513 samples according to the proposed hybrid filter. Its performances are little bit lower than that of both previous cases, yet Q_d levels are still high.

In Figs. 16–19 correspond to global error probability of the UFMC detection performance. For the same aforementioned design reason, Q_f ratios are also supposed to be as low as 0.01, 0.05, 0.07, and 0.1 for Figs. 16–19, respectively. In all figures, the global error probability is reduced with increasing the SUs number although the SNR is small due to the proposed hybrid filter.

Table 5 reveals the highest and the lowest values of the global probability of error for many ratios of the Q_f , SNR, and SUs number. It is easy to see that the Q_e is reduced when number of the SUs is increased unrelatedly to the SNR. Moreover, Q_e is high once SUs equal to 15 users but it deceases if the SUs >15 users.

Table 3Lowest and Highest Q_e of F-OFDM-5G Waveform.

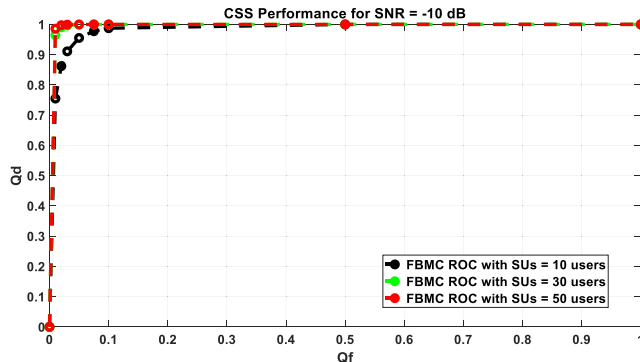
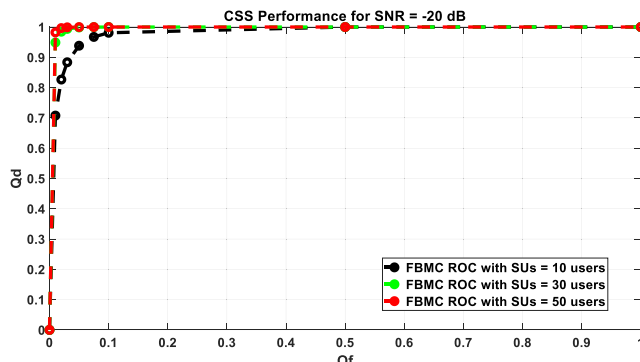
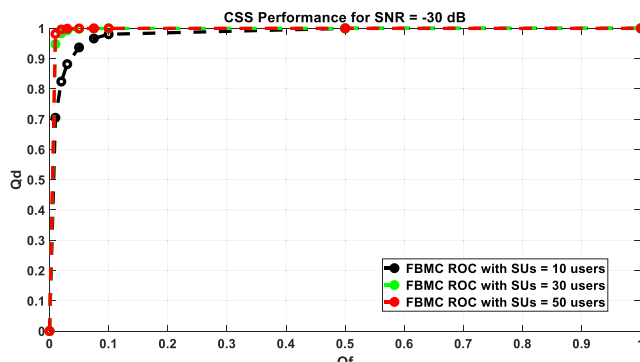
$Q_f = 0.01$		$Q_f = 0.05$		$Q_f = 0.07$		$Q_f = 0.1$	
Highest	Lowest	Highest	Lowest	Highest	Lowest	Highest	Lowest
Q_e	0.24451	0.02546	0.09012	0.05008	0.09113	0.07005	0.11388
SNR/dB	-5	-10	-20	-15	-30	-15	-10, -20
SUs No.	10	50	10	45	10	45	10

Fig. 13. UFMC Sensing for $\text{SNR} = -10 \text{ dB}$.Fig. 14. UFMC Sensing for $\text{SNR} = -20 \text{ dB}$.Fig. 15. UFMC Sensing for $\text{SNR} = -30 \text{ dB}$.Fig. 16. Q_e of UFMC for $Q_f = 0.01$.Fig. 17. Q_e of UFMC for $Q_f = 0.05$.Fig. 18. Q_e of UFMC for $Q_f = 0.07$.Fig. 19. Q_e of UFMC for $Q_f = 0.1$.**Table 4** Q_d of UFMC-5G Waveform for Given Q_f , SNR, and SUs Ratios.

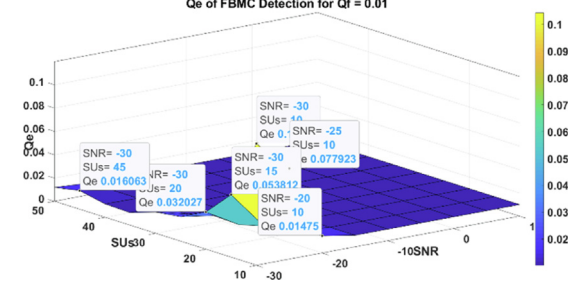
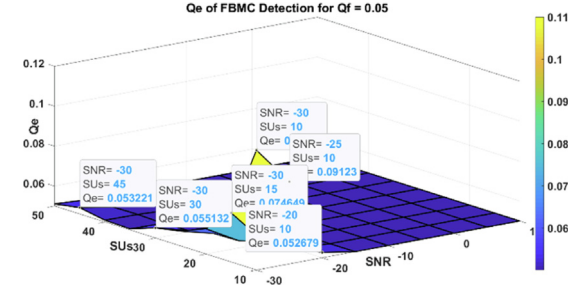
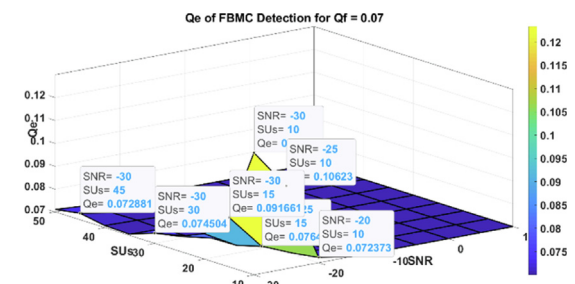
SUs No.	From Fig. 6	From Fig. 7	From Fig. 8
	SNR = -10 dB	SNR = -20 dB	SNR = -30 dB
10	$Q_d = 0.907$	$Q_d = 0.995$	$Q_d = 0.981$
30	$Q_d = 0.902$	$Q_d = 0.995$	$Q_d = 0.973$
50	$Q_d = 0.911$	$Q_d = 0.996$	$Q_d = 0.979$

Table 5Lowest and Highest Q_e of UFMG-5G Waveform.

	$Q_f = 0.01$		$Q_f = 0.05$		$Q_f = 0.07$		$Q_f = 0.1$	
	Highest	Lowest	Highest	Lowest	Highest	Lowest	Highest	Lowest
Q_e	0.072	0.013	0.054	0.05	0.071	0.07	0.1	0.1
SNR/dB	-20	-30	-20	-30	-20	-30	-20	-30
SUs No.	15	50	15	50	15	50	15	50

**Fig. 20.** FBMC Sensing for SNR = -10 dB.**Fig. 21.** FBMC Sensing for SNR = -20 dB.**Fig. 22.** FBMC Sensing for SNR = -30 dB.**Table 6** Q_d of FBMC-5G Waveform for Given Q_f , SNR, and SUs Ratios.

SUs No.	From Fig. 20	From Fig. 21	From Fig. 22
	SNR = -10 dB	SNR = -20 dB	SNR = -30 dB
10	$Q_d = 0.955$	$Q_d = 0.938$	$Q_d = 0.937$
30	$Q_d = 0.999$	$Q_d = 0.999$	$Q_d = 0.999$
50	$Q_d = 0.999$	$Q_d = 0.999$	$Q_d = 0.999$

Fig. 23. Q_e of FBMC for $Q_f = 0.01$.**Fig. 23.** Q_e of FBMC for $Q_f = 0.01$.**Fig. 24.** Q_e of FBMC for $Q_f = 0.05$.**Fig. 24.** Q_e of FBMC for $Q_f = 0.05$.**Fig. 25.** Q_e of FBMC for $Q_f = 0.07$.

4.4. Detection performance for FBMC-5G waveform

The last kind but not least, Figs. 20–22 reveal the ROC of detection performance for -10, -20, and -30 dB SNR, respectively, for FBMC-5G waveform kind. In Table 6, Q_d ratios are depicted for

0.05 global probability of false alarm, these ratios indicate that the updated length (3952 samples) is an optimum one. The ROCs in Fig. 20 are performed for 3952 samples, as against 4096 in the initial stream for SNR = -10 dB. The detection performance ratios

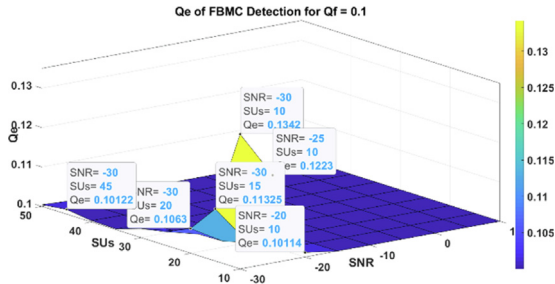


Fig. 26. Q_e of FBMC for $Q_f = 0.1$.

are large yet it is better when SUs >30 users. For SNR = -20 and -30 dB, Figs. 21 and 22 present the same detection performance of the previous case with 3915 samples for both cases. The performances for all cases are equal due to the signal stream is long.

The error of system is shown in Figs. 23–26 that correspond to detection system of the FBMC waveform kind. In all figures, the global error probability is the lowest due to the stream of the detected waveform is long. The proposed hybrid filter reduced the affection of low SNR.

The lowest and the highest ratios of Q_e are revealed in the Table 7 for various values of Q_f , SNR, and SUs number. The ratios of Q_e are too low due to the long of the detected signal and the proposed hybrid filter.

4.5. A comparison with related works

Table 8 describes a comparison of the proposed CSS techniques for the three various 5G waveforms to other related works. In this table, the related works are as follows: MMS is a Multi-Modal System [8], ADTA is an Adaptive Double-Threshold Algorithm [11], NMS is a NOMA-MIMO System [12], KFCM is a Kernel Fuzzy Clustering Model [13], PWA is a PSO-WOA Algorithm [15], and EMEF is an Eigen-value extraction and Maximum Entropy Fuzzy clustering algorithm [17].

As specified previously, the associated works were not feasible for SNR below -14 dB than increased global false alert probability. The system also exhibits higher computational complexity and is implementable for a single 5G waveform type. The proposed hybrid filter deals with several 5G waveform types and adheres to the CSS approach requirements for less complexity. Additionally, it has a small global false alert probability; concurrently, it has significant noise variance corresponding to distinct 5G waveforms.

Overall, as shown in Table 8, the FBMC scheme provides optimal results because it comprises a long sample stream. Short sensing time is critical for the UFMC waveform because of shorter streams. The F-OFDM balances the FBMC and UFMC approaches. On the other hand, from the previous graphical results, the F-OFDM is sensitive to varying of the SNR while the UFMC and FBMC are sensitive to varying of the number of SUs.

Table 7

Lowest and Highest Q_e of FBMC-5G Waveform.

$Q_f = 0.01$		$Q_f = 0.05$		$Q_f = 0.07$		$Q_f = 0.1$	
Highest	Lowest	Highest	Lowest	Highest	Lowest	Highest	Lowest
Q_e	0.104	0.011	0.11	0.051	0.123	0.072	0.134
SNR/dB	-30	-30	-30	-30	-30	-30	-30
SUs No.	10	50	10	50	10	50	10

Table 8

The Proposed CR-5G based CSS System Versus Related Works Comparison.

Parameters	Proposed Hybrid Filter for CSS			MMS [8]	ADTA [11]	NMS [12]	KFCM [13]	PWA [15]	EMF [17]
	F-OFDM	UFMC	FBMC						
SNR/dB	-30	-30	-30	-10	-14	0	-5	-5	-8
SUs No.	50	50	50	10	11	10	11	11	4
Q_f	0.01	0.01	0.01	0.2	0.05	0.98	0.1	0.1	0.1
Q_d	0.97	0.92	0.99	0.89	0.92	0.95	0.9	0.9	0.97
Q_e	0.03	0.08	0.01	0.31	0.13	0.97	0.2	0.2	0.13

5. Conclusion

A novel hybrid filter based CSS detection system for CR-5G network is implemented for a 5G environment case and comprises several waveform types as F-OFDM, UFMC, and FBMC since there is not system to sense all these kinds rather than one of them. It includes a cascaded stages of cosine filter, Welch segmentation, and Hamming windowing, where the proposed system provides effective detection abilities for all 5G waveform types. Moreover, the outcome of this study is superior to other associated works when compared using probabilities of detection and false alarm, computational complexity, and global system error. The best results of the proposed system are $Q_f = 0.01$, $Q_d = 0.979$, 0.929, and 0.999 for the F-OFDM, UFMC, and FBMC waveform kinds, respectively. In addition, the errors of global system are 0.031, 0.081, and 0.011 for the F-OFDM, UFMC, and FBMC waveform kinds, respectively. Thus, the detection performances of the proposed system are significant for all types of 5G waveforms. For future work opinion, it is possible to build the proposed system in various networks such as heterogeneous networks.

References

- [1] Al-Gharably M, Almutairi AF, Krishna A. Performance Analysis of the Two-Piecewise Linear Companding Technique on Filtered-OFDM Systems. *IEEE Access* 2021;9:48793–802. doi: <https://doi.org/10.1109/ACCESS.2021.3068371>.
- [2] Sakkas L, Stergiou E, Tsoumanis G, Angelis CT. 5G UFMC Scheme Performance with Different Numerologies. *Electronics* 2021;10(16):1915.
- [3] Demir, A.F., et al., "Waveform design for 5G and beyond," *arXiv preprint arXiv:1902.05999*, 2019, 10.1002/9781119333142.ch2
- [4] Song Z, Wang X, Liu Y, Zhang Z. Joint spectrum resource allocation in NOMA-based cognitive radio network with SWIPT. *IEEE Access* 2019;7:89594–603.
- [5] Akhtar MAK, Sahoo G. Enhancing cooperation in MANET using neighborhood compressive sensing mode. *Egyptian Informatics Journal* 2021;22(3):373–87. doi: <https://doi.org/10.1016/j.eij.2016.06.007>.
- [6] Kumar A, Sharma MK, Sengar K, Kumar S. NOMA based CR for QAM-64 and QAM-256. *Egyptian Informatics Journal* 2020;21(2):67–71.
- [7] Liu X, Jia M, Na Z, Lu W, Li F. Multi-modal cooperative spectrum sensing based on dempster-shafer fusion in 5G-based cognitive radio. *IEEE Access* 2018;6:199–208.
- [8] Kumar A, Tripta, Saha S. A decision confidence based multiuser MIMO cooperative spectrum sensing in CRNs. *Phys Commun* 2020;39:100995.
- [9] Lee W, Kim M, Cho D-H. Deep cooperative sensing: Cooperative spectrum sensing based on convolutional neural networks. *IEEE Trans Veh Technol* 2019;68(3):3005–9. doi: <https://doi.org/10.1109/TVT.2019.2891291>.
- [10] Yu S et al. Calibration program for the 16-foot antenna. *Wireless Communications and Mobile Computing* 2020. 2020.. doi: <https://doi.org/10.1155/2020/4794136>.
- [11] Balachander T, Krishnan M. Efficient Utilization of Cooperative Spectrum Sensing (CSS) in Cognitive Radio Network (CRN) Using Non-Orthogonal Multiple Access (NOMA). *Wireless Pers Commun* 2021;1:1–22. doi: <https://doi.org/10.1007/s11277-021-08776-7>.
- [12] Giri MK, Majumder S. Eigenvalue-based cooperative spectrum sensing using kernel fuzzy c-means clustering. *Digital Signal Process* 2021;111:. doi: <https://doi.org/10.1016/j.dsp.2021.102996>.
- [13] Kansal P, Gangadharappa M, Kumar A. An Efficient Composite Two-Tier Threshold Cooperative Spectrum Sensing Technique for 5G Systems. *Arabian Journal for Science and Engineering* 2022;47(3):2865–79.
- [14] Gupta V, Beniwal NS, Singh KK, Sharan SN, Singh A. Optimal cooperative spectrum sensing for 5G cognitive networks using evolutionary algorithms. *Peer-to-Peer Networking and Applications* 2021;14(5):3213–24.
- [15] Yli-Kaakinen J et al. Frequency-Domain Signal Processing for Spectrally-Enhanced CP-OFDM Waveforms in 5G New Radio. *IEEE Trans Wireless Commun* 2021. doi: <https://doi.org/10.1109/TWC.2021.3077762>.
- [16] Costa, Lucas Dos Santos, Dayan Adionel GUIMARÃES, and Bartolomeu F. Uchôa-Filho. "On the Signal-to-Noise Ratio Wall of Energy Detection in Spectrum Sensing." *IEEE Access* 10 (2022): 16499–16511. 10.1109/ACCESS.2022.3149476
- [17] Giri MK, Majumder S. "On eigenvalue-based cooperative spectrum sensing using feature extraction and maximum entropy fuzzy clustering". *J Ambient Intell Hum Comput* 2022;1:1–15. doi: <https://doi.org/10.1007/s12652-021-03670-3>.
- [18] Kong D, Zheng X, Zhang Y, Jiang T. Frame repetition: A solution to imaginary interference cancellation in FBMC/OQAM systems. *IEEE Trans Signal Process* 2020;68:1259–73. doi: <https://doi.org/10.1109/TSP.2020.2971185>.
- [19] Chen H, Hua J, Wen J, Zhou K, Li J, Wang D, et al. Uplink interference analysis of F-OFDM systems under non-ideal synchronization. *IEEE Trans Veh Technol* 2020;69(12):15500–17. doi: <https://doi.org/10.1109/TVT.2020.3041938>.
- [20] Guo Z, Liu Q, Zhang W, Wang S. Low complexity implementation of universal filtered multi-carrier transmitter. *IEEE Access* 2020;8:24799–807. doi: <https://doi.org/10.1109/ACCESS.2020.2970722>.
- [21] Vega A, Alejandro E, Orozco ALS, Villalba LJG, Hernandez-Castro J. Digital images authentication technique based on dwt, dct and local binary patterns. *Sensors* 2018;18(10):3372. doi: <https://doi.org/10.3390/s18103372>.
- [22] Salman EH, Noordin NK, Hashim SJ, Hashim F, Ng CK. An analysis of periodogram based on a discrete cosine transform for spectrum sensing. *Wireless Pers Commun* 2018;101(3):1261–79.
- [23] Hua Z, Zhou Y, Huang H. Cosine-transform-based chaotic system for image encryption. *Inf Sci* 2019;480:403–19. doi: <https://doi.org/10.1016/j.ins.2018.12.048>.
- [24] Kim JK, Ahn JM. Effects of a spectral window on frequency domain HRV parameters. In: In Advances in Computer Communication and Computational Sciences. Singapore: Springer; 2019. p. 697–710. doi: https://doi.org/10.1007/978-981-13-6861-5_59.
- [25] Hampannavar, Santoshkumar, C. Bhanu Teja, M. Swapna, and Uday Kumar RY, "Performance Improvement of M-Class Phasor Measurement Unit (PMU) using Hamming and Blackman Windows," *IEEE International Conference on Power Electronics, Smart Grid and Renewable Energy (PESGRE2020)*, pp. 1–5. IEEE, 2020. 10.1109/PESGRE45664.2020.9070382